TESLA Report 2001-34

DESY, November 2001

Bulk and Grain Boundary Diffusion of Titanium in High Purity Niobium

A.Bernasik, K.Kowalski

Surface Spectroscopy Laboratory
University of Mining and Metallurgy
Krakow, Poland

X.Singer, W.Singer

DESY

1. Introduction

The TESLA cavities based on niobium are continuously investigated to improve their properties. In order to reach their high operating parameters such as gradient field over 25 MV/m each step of fabrication have to be rigorous controlled. One of the most important problems is the presence of impurities which have strong impact on the deterioration of the superconducting properties. Dissolved gases act as scattering centres for unpaired electrons and reduce the thermal conductivity. Therefore, the niobium cavities are out-gased in the procedure called solid state gettering. The niobium cavities are heat-treated for several hours at high temperature (up to 1400ºC) in the vacuum furnace in the presence of pure Ti plates uniformly placed around the cavity. During this process the vapour deposited Ti layer continuously grows on and simultaneously diffuses into the niobium substrate. At the end of the process the Ti thickness reaches about hundred microns. The deposited layer plays a role of getter, which purifies the niobium from dissolved gases such as hydrogen, nitrogen, oxygen or carbon. After this procedure the titanium is removed from the surface of the quenched cavity. This is done chemically in acid mixtures. To remove the whole quantity of titanium not only the thickness of the deposited Ti layer must be known but also the penetration depth of Ti in the Nb substrate should be evaluated. This depth depends on the bulk (lattice) diffusion inside Nb grains as well as on the grain boundary diffusion.

The aim of this work is to study the transport of Ti in Nb during the vapour deposition process at different conditions. This purpose can be achieved using adequately sensitive depth profiling method. In this work the Secondary Ion Mass Spectrometry was adopted.

2. Experimental

2.1 Niobium samples and properties

Several Nb samples were annealed at different temperatures (800°C, 1000°C, 1200°C, 1400°C) for 4 hours with Ti and without Ti. Niobium of three companies, that supplied material for TTF (HERAEUS, Wah Chang (TWC) and Tokyo Denkai(TD)) were tested. The mechanical properties, microstructure and RRR are analysed. Some results can be seen in Fig. 2.1-2.6.

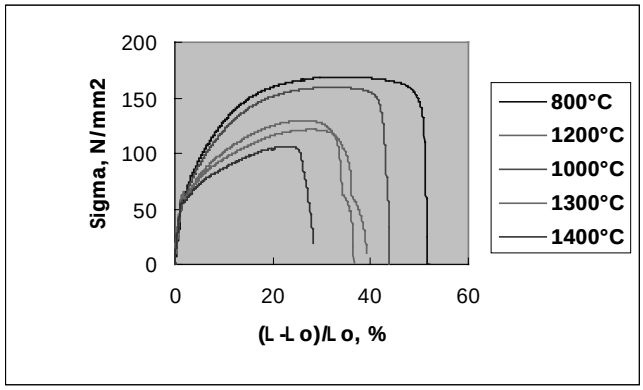

Fig.2.1. Strain-stress curves of HERAEUS Nb

The typical result of tensile test represents Fig 2.1. The stress-strain curves show, that raising the annealing temperature from 800°C to 1400°C reduces the breaking elongation and the tensile strength almost by a factor of two. A big difference between annealing with Ti and without Ti was observed in the region of transition from elastic to plastic behaviour (Fig. 2.2-2.3).

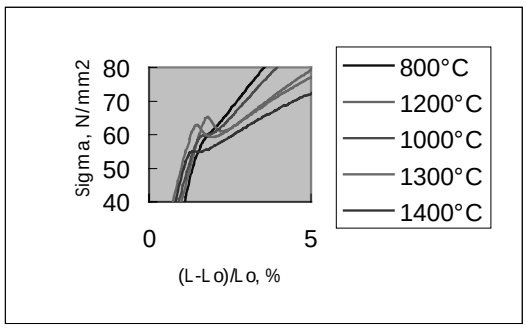

Fig. 2.2. Strain-stress curves of HERAEUS Nb, annealed at different temperatures 4h with Ti

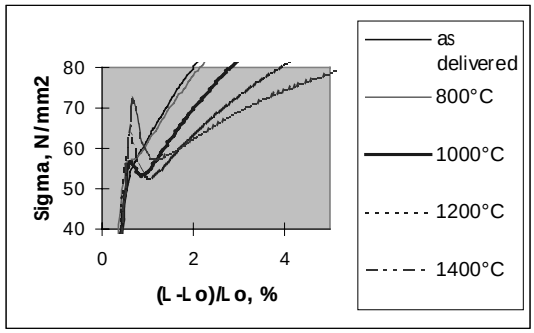

Fig. 2.3. Strain-stress curves of HERAEUS Nb, annealed at different temperatures 4h without Ti

The upper and lower yield point can be clearly seen in both cases. Such strain-stress curves are typical for body centred cubic metals like Nb, if it contains traces of interstitial impurity atoms. This fact suggests that the dislocations are strongly pinned by impurity atoms. Impurity atoms, which differ in size from the host atoms of a lattice are diffused to a dislocation line and create close to it a so called impurity cloud. The impurity cloud pins the dislocation and makes its motion difficult. The upper yield point can be explained as a stress needed for breaking the dislocations away from the impurity clouds. Free from a cloud the dislocation can move at a lower stress level, which presents the lower yield point.

The annealing with Ti reduces the concentration of interstitial impurities and, in a good accordance with pinning mechanism, reduces the difference between upper and lower yield points by increasing of annealing temperature. On the contrary the annealing without Ti increases the content of interstitial impurities and the ratio of the upper to the lower yield point. These results shows, that a qualitative conclusion about grade of Nb purity can be drown from the behaviour of it stress-strain characteristic.

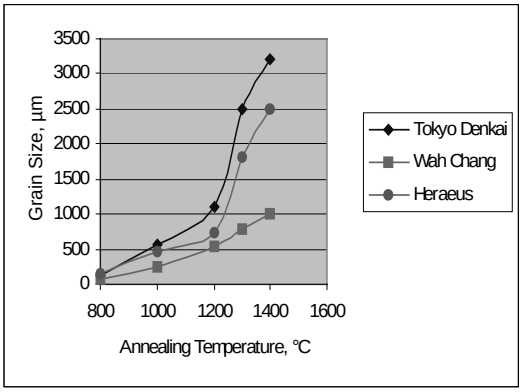

Fig. 2.4. Grain size versus the annealing temperature for Nb of different suppliers

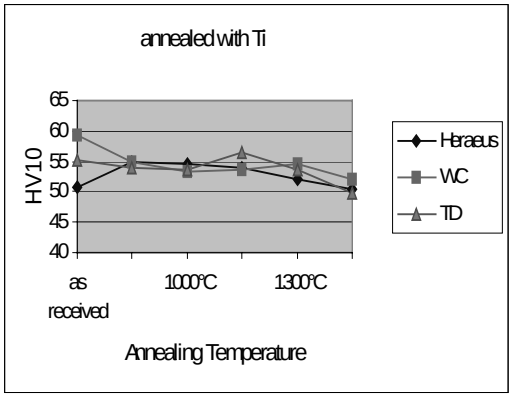

Fig. 2.5. Hardness HV10 versus the annealing temperature for Nb of different suppliers

The grain growth during annealing of the Nb of different suppliers can be seen in Fig. 2.4. The essential growth of the grain starts at 1000°C. It is interesting to notice a correlation between the diameter of the Nb ingot and the grain size in the sheet (the grain size is proportional to 1/D, where D is the ingot diameter).

The behaviour of the hardness HV10 during annealing with Ti and without Ti is represented by Fig. 2.5. The hardness almost does not change with grain growth. Only at high annealing temperatures, when the difference in purity becomes significant, the hardness weakly decreases or increases for samples annealed with Ti or without Ti, respectively.

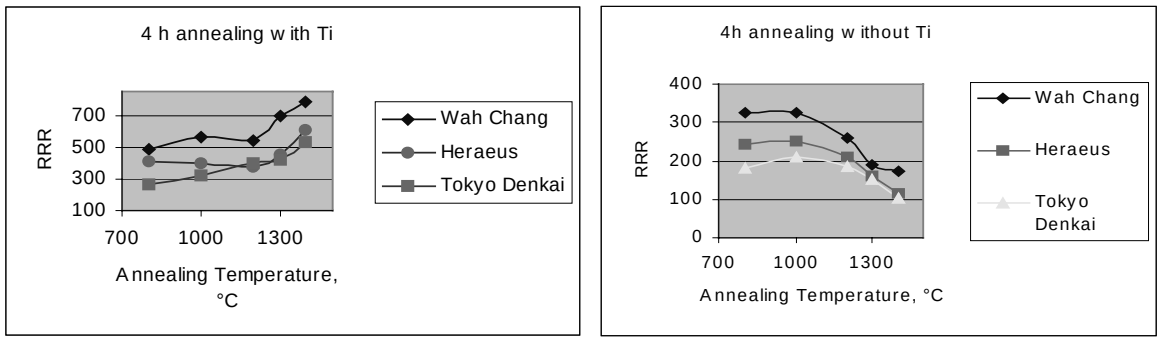

Fig. 2.6 RRR versus the annealing temperature for Nb of different suppliers.

The tendency of RRR behaviour is similar for Nb of all tree suppliers. Evidently, the annealing with Ti increases the RRR (Fig. 2.6) and annealing without Ti reduces it. The significant changes of RRR starts from 1000-1200°C.

2.2 Depth profiling methods

Conventional profiling method based on angle lapping is usually used for sampling depth over several μm. In this method sample is cut and polished at well definite angle. Such prepared surface displays the distribution of elements in depth of the sample and it is mostly analysed by EDX or Auger microscopy. A special case of this method is a ball cratering where the angle lapping is replaced by using rotating steel ball coated with fine diamond paste.

More sensitive technique with better depth resolution than mechanical abrasion is an ion sputter profiling. This method is recommended for depth smaller than 2 μm. Here as analytical tools Auger microscopy or SIMS are typically applied.

2.3. SIMS method.

Secondary Ion Mass Spectrometry is based on sputtering phenomenon. Primary ions beam with energy in the range from 1 to 30 keV eject from the surface atoms, ions or clusters at different state of ionisation. In the mass spectrometer only charged particle can be detect, therefore process of ionisation at the sample surface play fundamental role in this method. Number of ejected ions per the primary ion strongly depends on chemical composition of the surface. For example, the presence of oxygen on the surface of certain metals can increase

ionisation probability of ejected atoms even four orders of magnitude. This so called matrix effect makes great difficulties in the determination of absolute value of concentration. Although some elements of very low concentration can be easily detected.

Using SIMS method four types of information can be obtained. Mass spectra allows determining isotopic composition of the sample surface. Depth profiling informs about distribution of elements (isotopes) in depth. Composition maps illustrate lateral distribution of elements (isotopes) on the surface . Successive maps collected vs time of sputtering inform about a spatial distribution of the elements. During ion bombardment not only particles but also electrons are ejected. Its intensity inform about the topography of the sample surface similar to conventional SEM microscopy.

2.4. SIMS analysis

SIMS measurements were determined in a Vacuum Scientific Workshop Ltd. apparatus under pressure less then 5×10^{-8} mbar. Sample surface was sputtered using double lens liquid metal ion beam gun (FEI Company) which allowed to accelerate Ga^+ primary beam ions to energy of 25 keV. The current of the primary ion beam was in the range from 1 to 4 nA. Sputtered area was chosen depending on necessity and varied from 20×20 μm to 1×1 mm. In depth profiling only the ions coming from the central 40% of crater area were analysed to avoid the undesirable edge effect. Secondary ions were detected in the Balzers quadrupole mass spectrometer. Using optimal parameters depth resolution of about 10 nm and lateral distribution of about 120 nm can be achived.

The depth scale was calculated from sputtering parameters (time of sputtering, primary ion current, sputtered area) and a sputter yield. The sputter yield was determined in independent experiments by measuring the depth of the crater sputtered at controlled conditions (known the sputtering parameters). It was assumed that Nb and Ti sputter yields are equal. The thickness of the measured layers were established at the depth where the Ti intensity decreased to 10% of its value in the layer.

3. Results and discussion

3.1 Comparison of EDX with SIMS analysis

Analysis of thick layers is usually performed using the angle lapping method combined with EDX as an analytical tool. Here, introductory experiments were carried out in order to verify sensitivity of the SIMS method by comparing the results with those obtained by EDX. For these experiments the pure niobium plate with the Ti layer of about 40 μm deposited at high temperature was cut perpendicularly to the surface and then polished. The cross-section was analysed by two methods: EDX and SIMS. For both elements Ti and Nb, composition maps and linescanes across the Ti layer were acquired at standard conditions (reasonable time of acquisition). Results are shown in Figs. 3.1 and 3.2 for EDX and SIMS, respectively.

Presented results indicate that accuracy of Ti and Nb detection is better in the SIMS method. Both methods illustrate comparable distribution of Ti in the layer but the SIMS composition maps show higher contrast and the SIMS linscans are less noisily.

High sensitivity of SIMS method allows measuring signal for ratio m/q of 48 not only in the Ti layer but also in niobium region (see linescan in logarithmic scale in Fig. 3.2). Titanium can be expected here for two reasons: Ti diffusion into Nb or smearing during the cut or polishing procedure. Although this signal could be attributed to titanium it needs precise verification. This is the subject of the next paragraph.

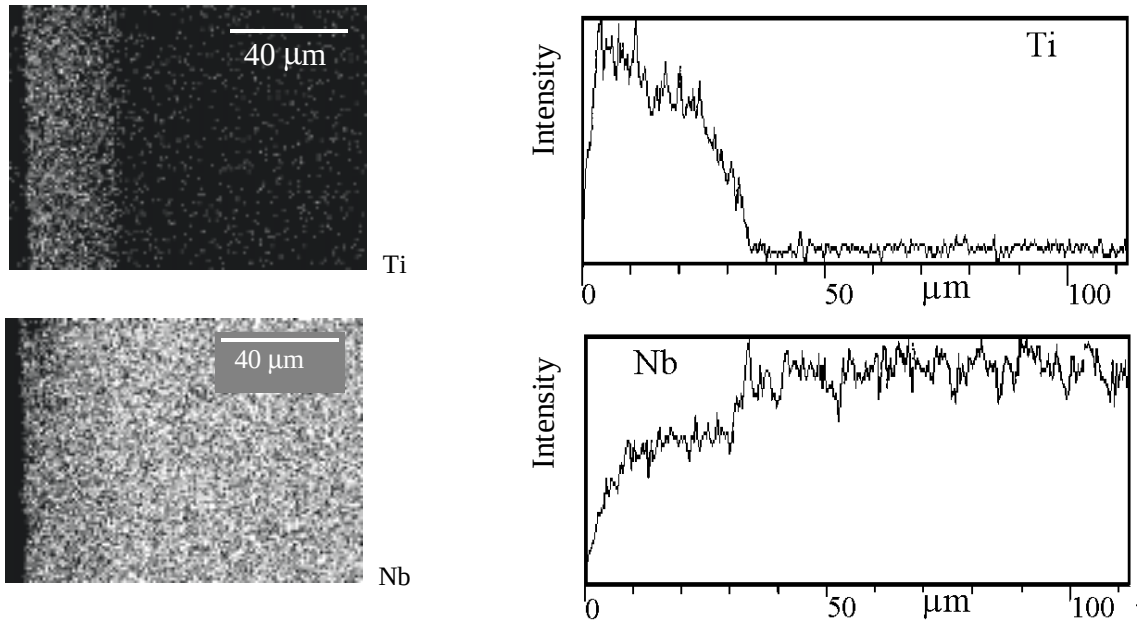

Fig. 3.1. EDX composition maps and linescanes measured on the cross-section of pure niobium plate covered by thick Ti layer. Intensity axes of the linscans are plotted in the linear scale.

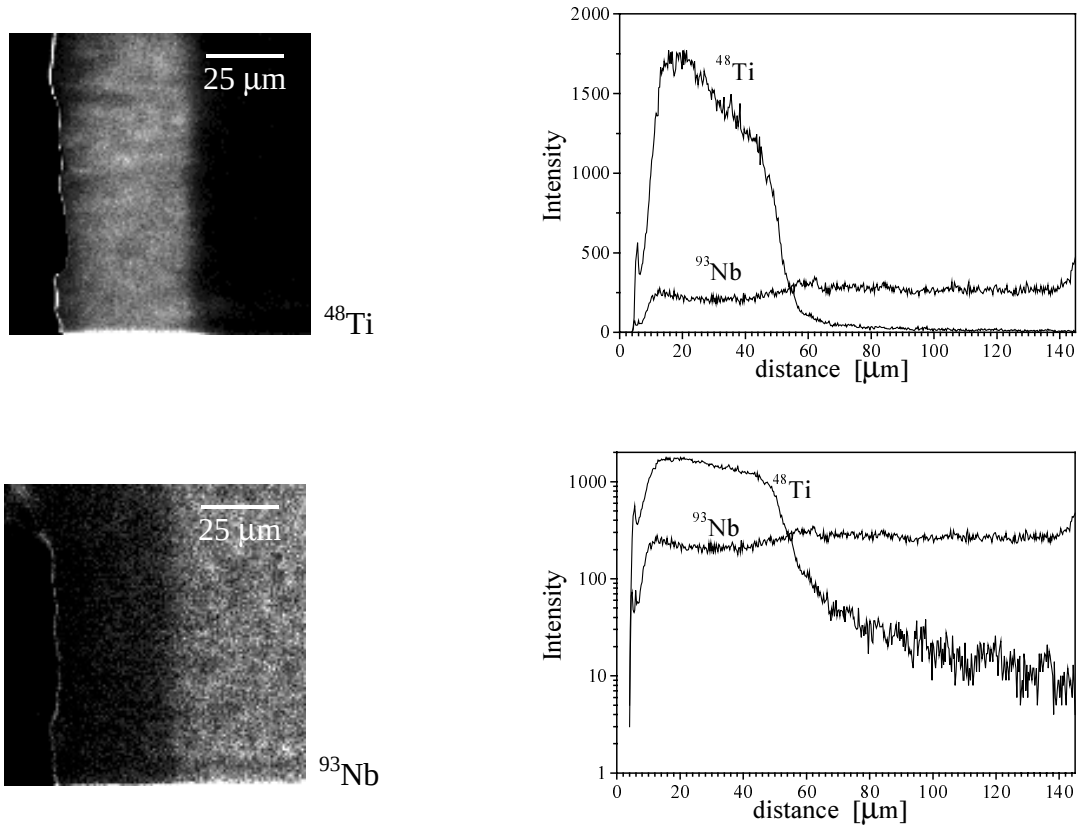

Fig. 3.2. SIMS composition maps and linescanes measured on the cross-section of the pure niobium plate covered by thick Ti layer. Presentation of the linescans relates to the same data but plotted in linear and logarithmic scale, respectively.

3.2. Elements identification in the SIMS mass spectra.

In order to determine true profiles or composition maps it is important to verify whether measured signals correspond to chosen elements. This uncertainty can appear due to overlapping of measured peaks of the same mass to charge ratio (m/q) coming from different ions or clusters. It is more important for the samples containing several elements. Such problem usually appears when the surface of the analysed samples is contaminated.

Fig. 3.3 illustrates the mass spectra for m/q from 1 to 400 amu measured for TWC sample treated at 1000^{o}C where only Ti and Nb were expected. The analysis showed presence of such elements as Na, Si, K, and Ca. The composition maps and mass spectra for HERAEUS sample treated at the same temperature (Fig. 3.4) show that the impurities were not distributed homogeneously and identification of titanium was difficult. Composition maps for this sample and also for the TD sample treated at 1400^{o}C (Fig. 3.5) indicate that the impurities were located in pores. Depth profile measured for such contaminated samples (Fig. 3.5) can represent only average concentration. These results lead to the conclusion that to correct determination of titanium the samples for analysis should be stored and transported with great care to avoid any contamination. Next experiments show that on clean surface even very low intensity can be referred to titanium.

Mass spectra for a sample with low impurities concentration at the surface are presented in Fig 3.6 where the main elements: titanium and niobium can be easily identifed. Titanium appears on mass spectra at m/q equal to 46, 47, 48, 49, 50 with intensity proportional to the abundance 8.0, 7.3, 73.8, 5.5, 5.4, respectively. Niobium which has only one isotope is detected at 93. Analysis of deeper layer shows drastic reduction of Ti peaks but they are still detectable. For both spectra the intensity of Nb remains nearly constant. To eliminate edge effect the second spectra was registered inside the crater sputtered during the first spectra analysis.

The analysis inside the crater was usually done to verify whether the measured signal in depth profiling or the compositional maps acquisition corresponded to chosen element. An example of such verification procedure is presented in Fig 3.7. For the depth profile obtained for the niobium sample covered by 30 nm Ti layer and then annealed at 1400^{o}C for 75 min, the intensity for m/q 48 was very low. Therefore the measurement was interrupted and mass spectra was acquired. The spectra indicate that the intensity corresponds to titanium. These verification measurements were employed as routine procedure in the experiments in this work.

a)

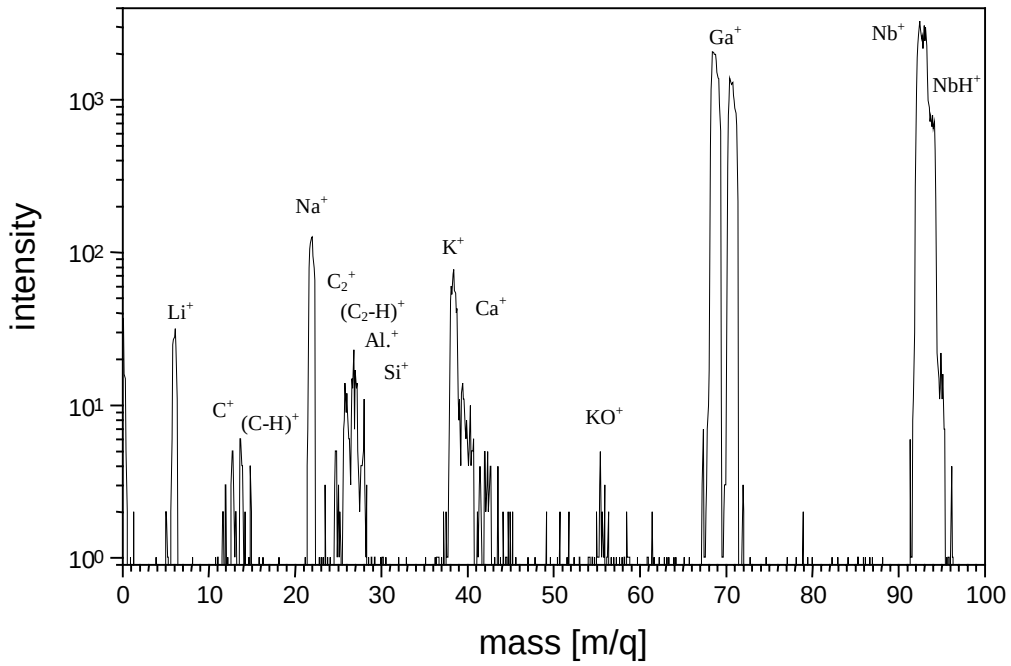
intensity
mass [m/q]
Li+
C+
(C-H)+
Na+
C2+
(C2-H)+
Al.+
Si+
K+
Ca+
KO+
Ga+
Nb+
NbH+

b)

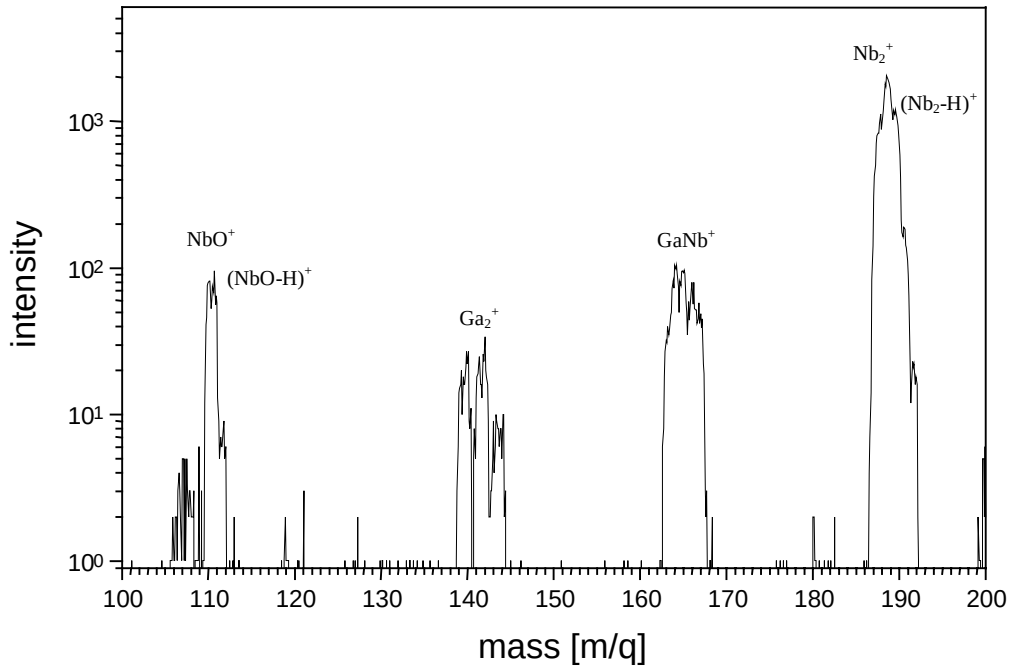
intensity
mass [m/q]
NbO+
(NbO-H)+
Ga2+
GaNb+
Nb2+
(Nb2-H)+

c)

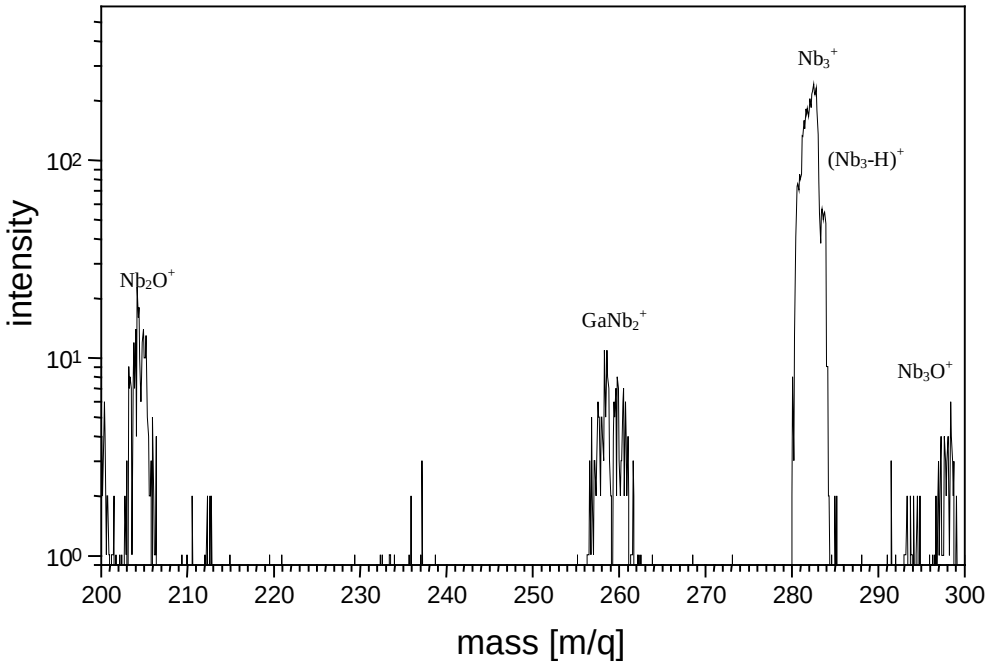

d)

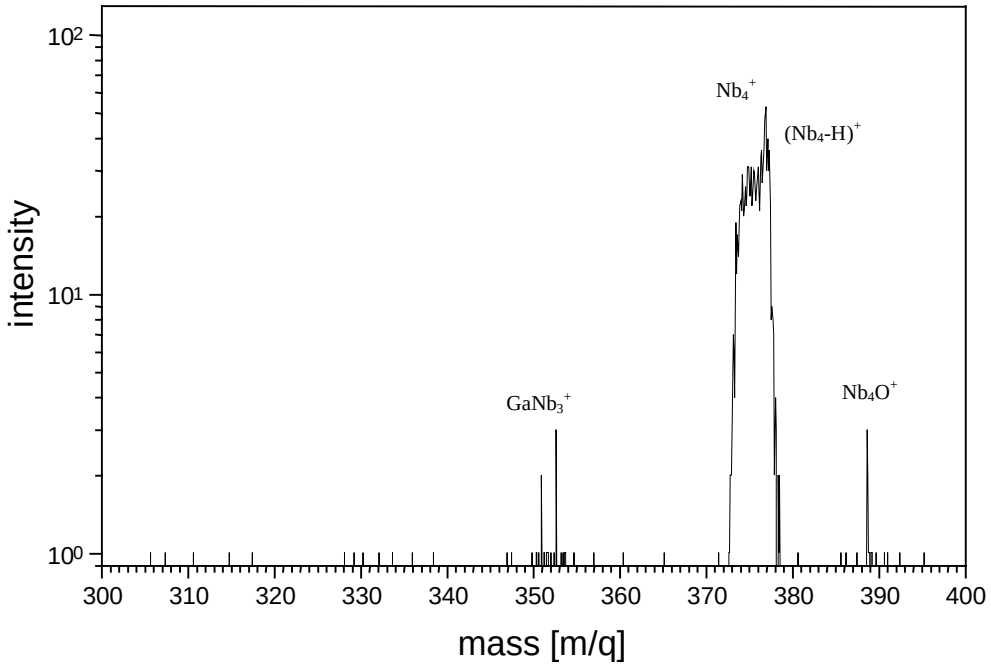

Fig. 3.3. SIMS mass spectra of positive ions for the TWC sample treated at 1000^{o}C.

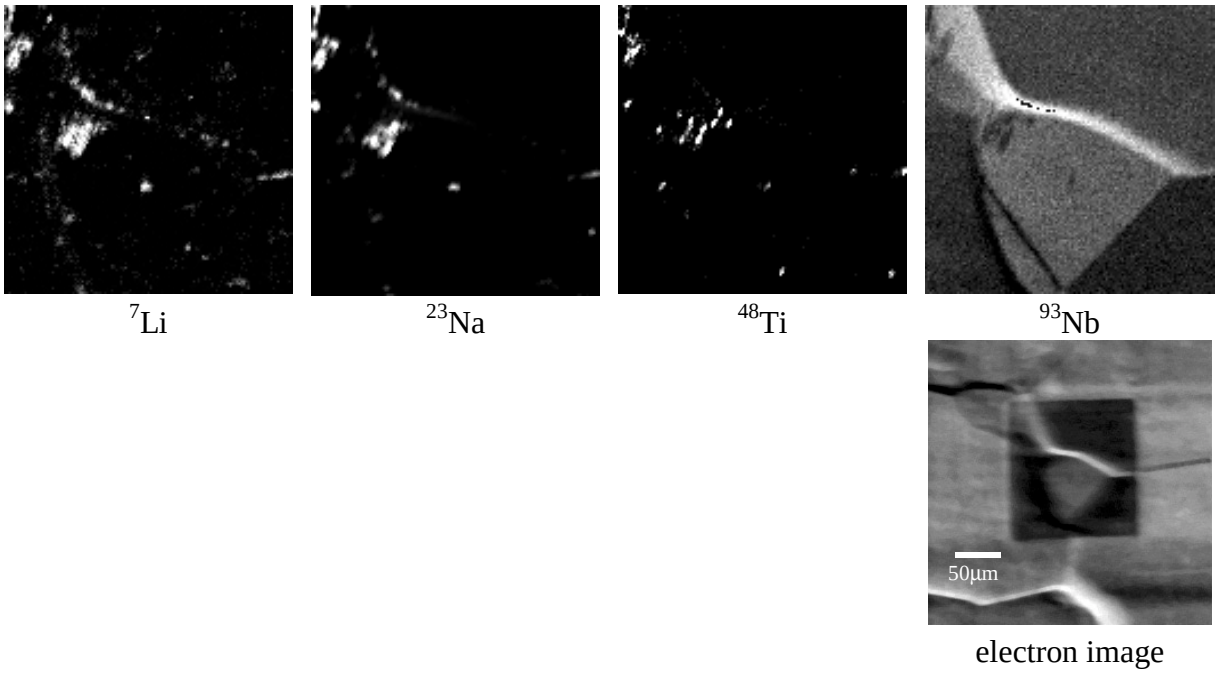

Fig. 3.4. Composition maps and titanium region mass spectra measured for the sample HERAEUS treated at 1000°C. Identification of titanium is difficult because of the presence of the impurities at the sample surface.

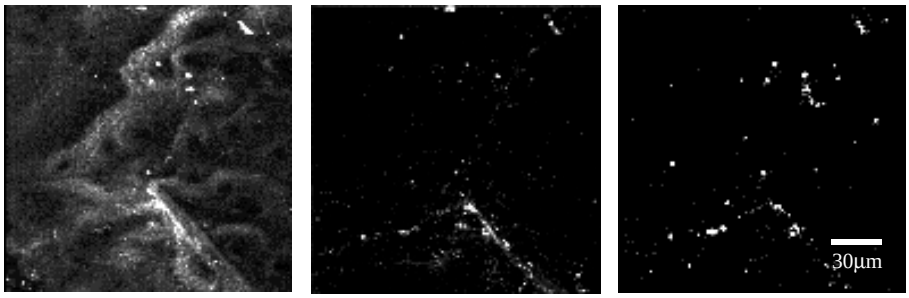

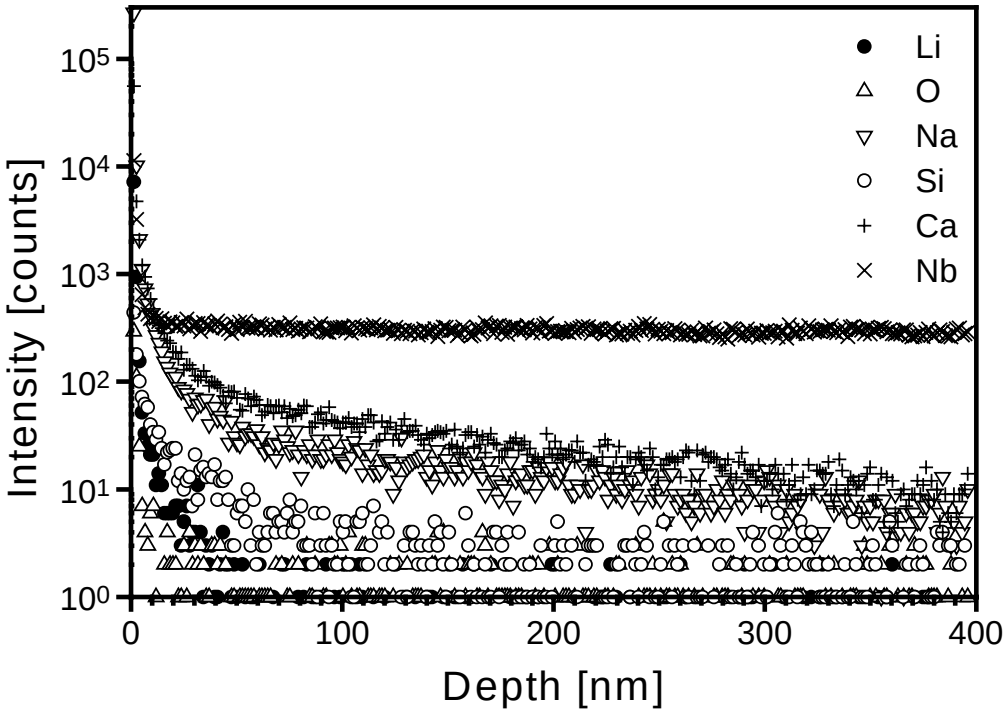

Fig. 3.5. Composition maps and depth profile of the impurities measured for the sample TD treated at 1400°C.

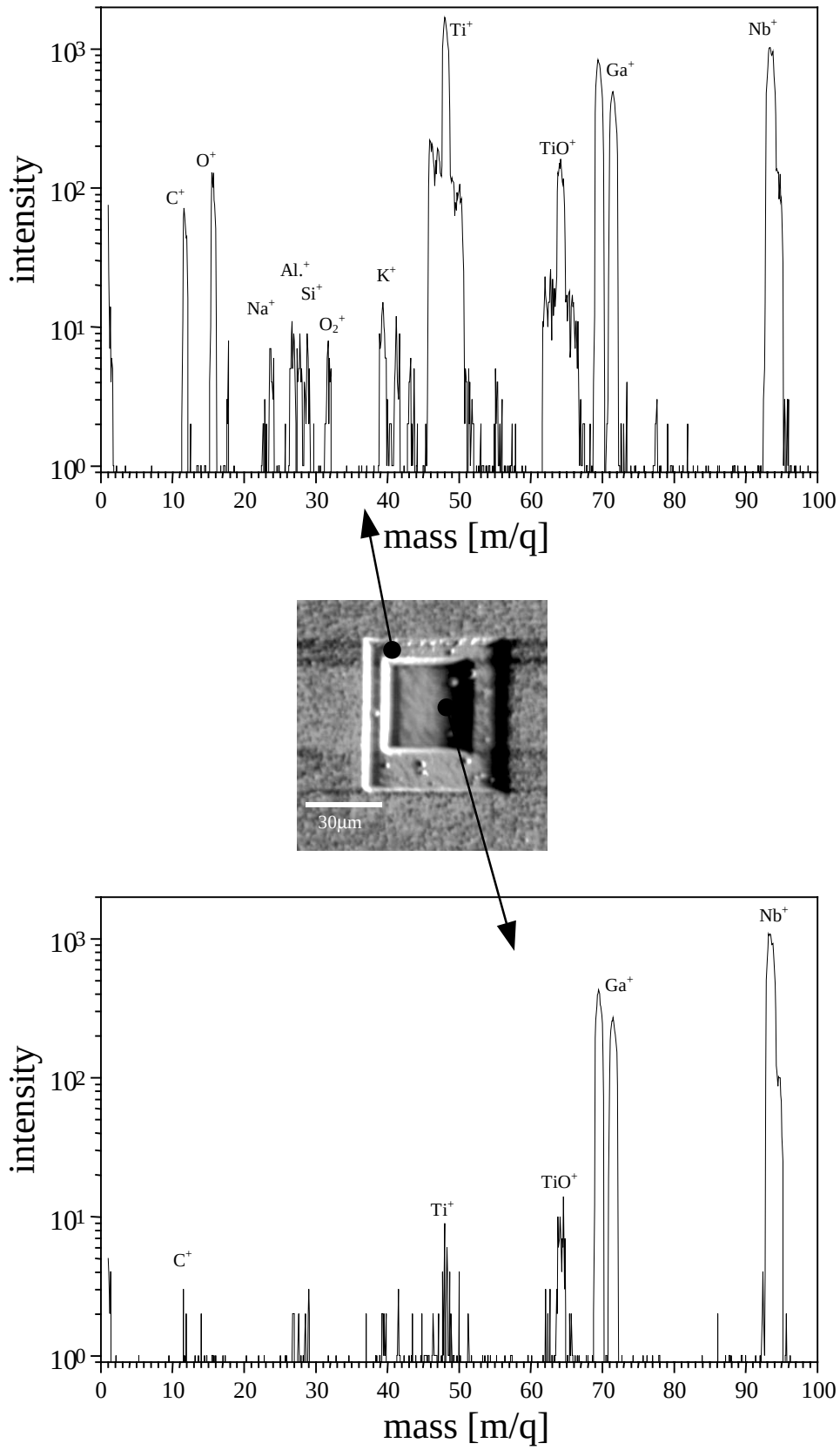

Fig 3.6. Comparison of mass spectra measured at the surface and in the deeper layer for the niobium sample with Ti layer of 30 nm annealed at 1200^{o}C for 2h.

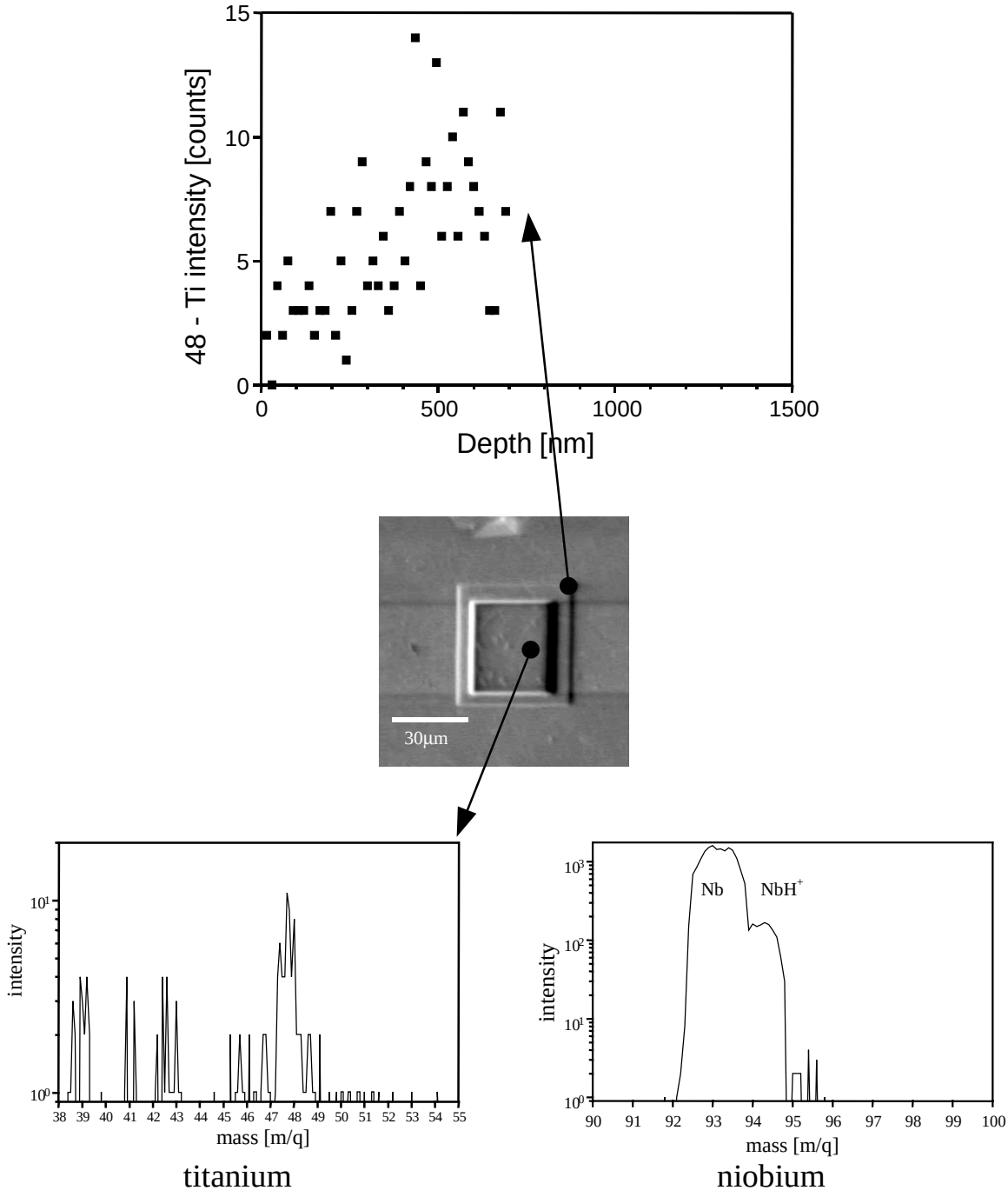

Fig. 3.7. Verification of the signal measured during depth profiling for the niobium sample with Ti layer of 30 nm annealed at 1400°C for 75 min.

3.3. Thickness of the Ti vapour deposited overcoat

Thickness of titanium deposited on niobium strongly varies with the temperature and it is difficult to evaluate this value using only one method. Therefore the depth profiling, mapping on the cross-sections and ball cratering analysis were employed. For all of them SIMS was used as an analytical tool. In these experiments two sets of pure niobium samples were used and named accordingly to their producers: TWC and HERAEUS. The coating procedure were performed at 800, 1000, 1200, 1300 and 1400^{o}C.

Results for the TWC samples are collected in Fig. 3.8.

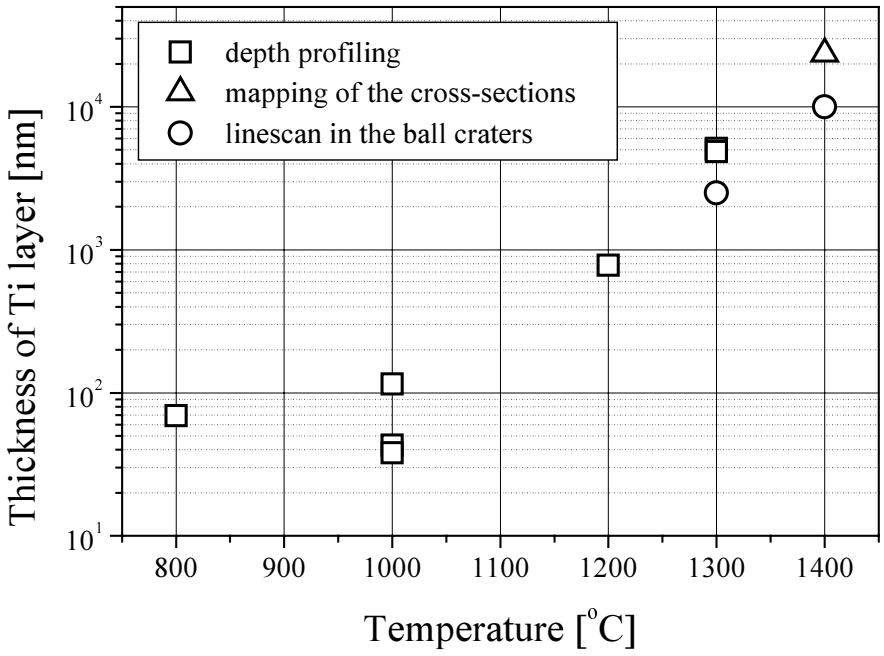

Fig. 3.8. Thickness of the Ti layer deposited at different temperatures on niobium (TWC) support evaluated by different methods.

Thickness of the layers thinner than 5 μm were evaluated by the depth profiling what allowed measuring the layer for the samples treated up to 1300^{o}C. This method did not provide satisfactory results for the sample with the thickest Ti layer obtained after treatment at 1400^{o}C. The depth profiles and the electron images which illustrate topography of analysed area are presented in Fig. 3.9.

Titanium vapour-deposition at low temperatures (800°C and 1000°C) formed the Ti layer of the thickness of about 100 nm. High scatter of experimental points for the sample annealed at 1000°C was induced by relatively large analysed area (100×100μm^2) that covered

several grains. For these samples, with thin Ti layer and small grains, it was not possible to perform analysis on one grain, because with reducing of the sputter area drastically increases the sputter rate and the Ti layer could not be detected. The profile for the sample treated at 1000°C compared to the sample treated at 800°C do not present sharp interface between the Ti layer and Nb (see Fig. 3.9). This can be explained by higher Ti diffusion into Nb than increasing of the thickness of the Ti layer. Higher Ti and Nb intensities in near surface region (at the depth lower than 10 nm) can be explained by the presence of surface oxide layer. Oxygen drastically increases ionisation probability of sputtered atoms (matrix effect). Analysis of the layers deeper than 2 μm showed characteristic decreasing of the Nb intensity. This effect was induced by trapping the secondary ions ejected from bottom on walls of the crater.

Electron images clearly indicate changes of the surface topography with temperature of deposition. Grain size increases with temperature and some of the grains outgrow from the surface. Depth profiles indicate that for top and bottom grains the thickness of the Ti layer were the same.

The cross-sections were performed for the samples prepared at 1200, 1300 and 1400°C but acceptable results were obtained only for the sample treated at the highest temperature. Here the thickness was estimated to about 23 μm (Fig. 3.10). For this set of the samples the ball cratering method was also applied. The thickness was estimated to about 2 μm and 10 μm for the samples annealed at 1300 and 1400°C respectively. Analysis of the ball crater for the sample treated at 1200°C did not give satisfactory results.

The sputter profiling method was applied also to the HERAEUS samples coated at 1200 and 1300°C. The thickness of the Ti layers were similar to that measured for TWC samples and were estimated to about 0.7 (see Fig. 3.11) and 6 μm respectively to the temperatures.

For both TWC and HERAEUS sets of samples it was observed that the Ti intensities did not fall to zero but for long time of sputtering remained constant. This observation suggest that some amount of titanium diffused into deeper part of the sample through fast diffusion paths. To confirm this presumption accurate experiments with different Ti isotopes were performed. As it is shown in Fig. 3.11 intensities of three isotopes changed in the same manner. Moreover, mass spectra measured at the surface before depth profiling and in the central part of the bottom of the crater indicate presence of titanium. Penetration of titanium in niobium is of interest in next two paragraphs.

800°C

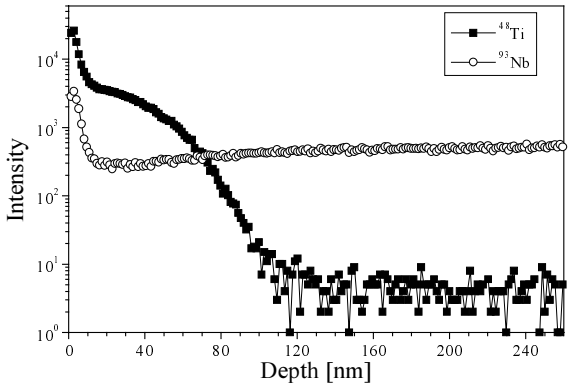

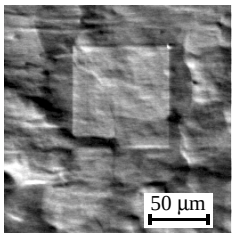

1000°C

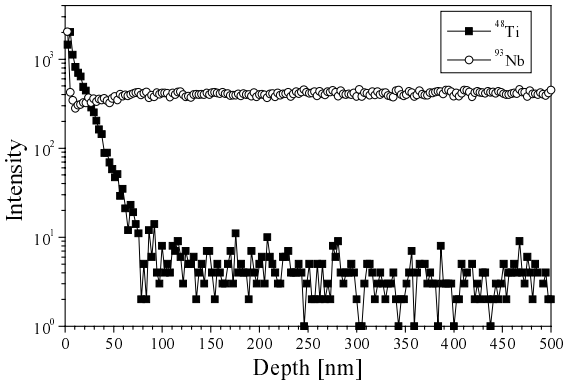

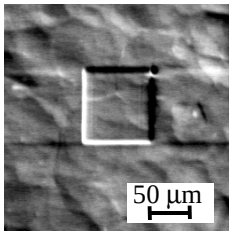

1200°C

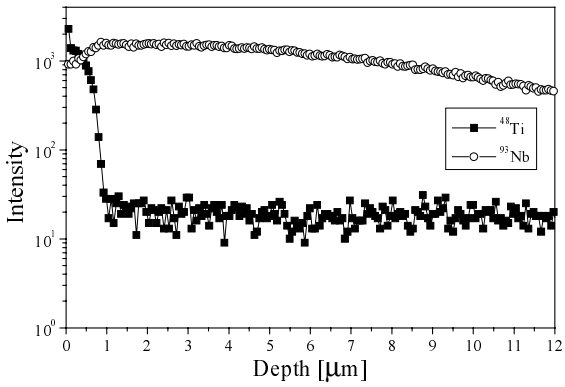

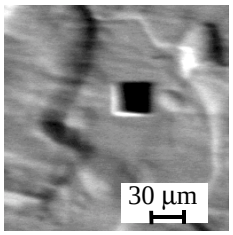

1300°C

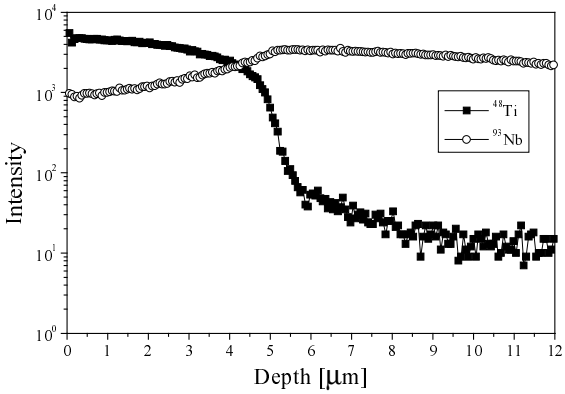

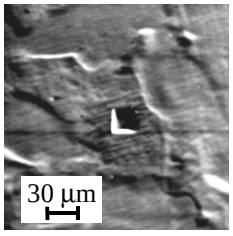

Fig. 3.9. Ti and Nb depth profiles measured on the sample treated at different temperatures. Electron images show the topography of the analysed area and the craters after depth profiling.

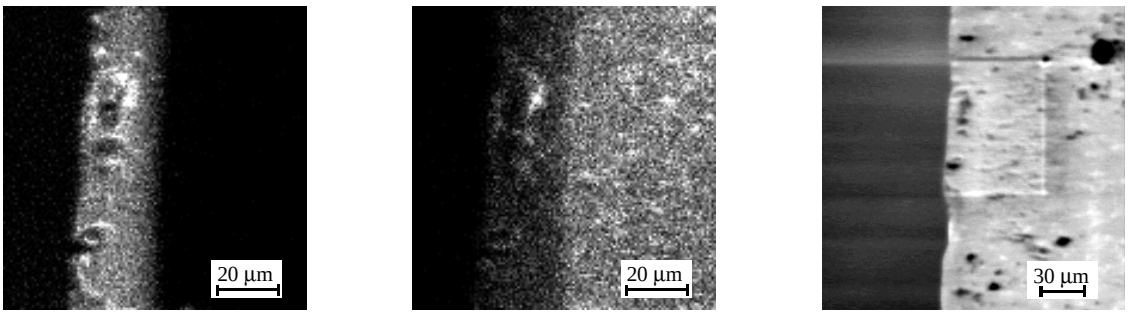

^{48}Ti ^{93}Nb electron image

Fig. 3.10. Composition maps of the cross-section for the TWC support coated by titanium at 1400°C. Electron image shows topography of edge of the sample and analysed area.

a) before depth profiling

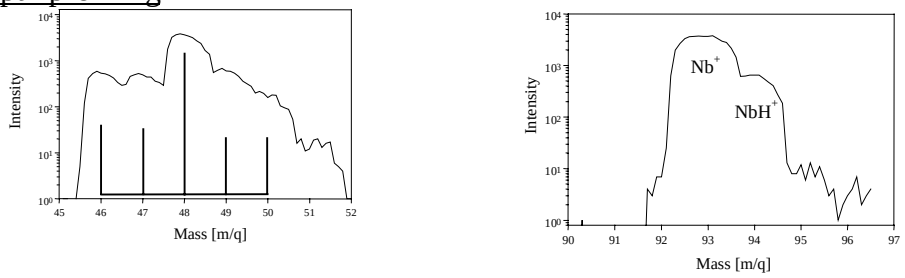

titanium niobium

b) depth profile

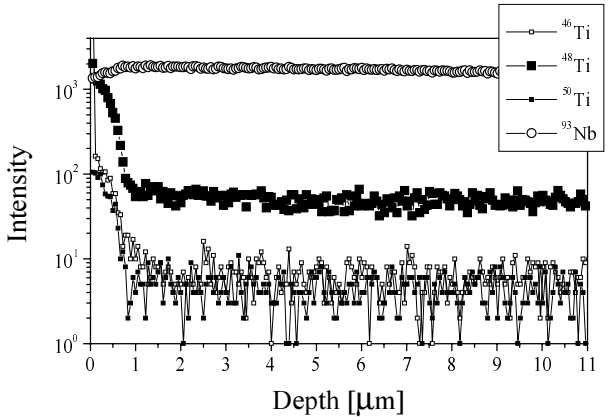

c) after depth profiling

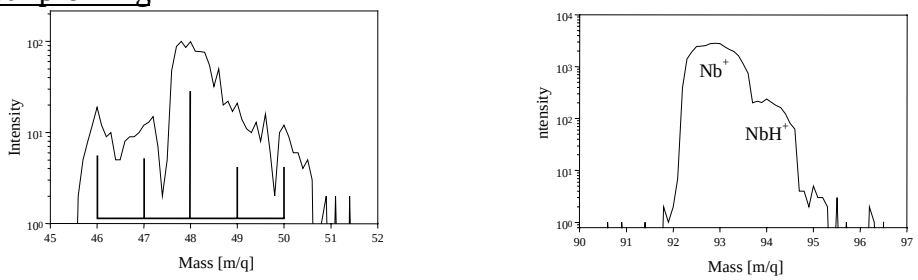

titanium niobium

Fig. 3.11. Depth profile and mass spectra (low resolution) measured on the HERAEUS sample vapour-coated at 1200°C. The spectra obtained after depth profiling were measured in the central of the crater.

3.4. Determination of the Ti bulk diffusion coefficient in niobium

The knowledge of the bulk and grain boundary diffusion coefficients of titanium in niobium is necessary to control the penetration depth of Ti during the purification heat treatment of the niobium cavities. Unfortunately, the relatively great thickness of the vapour deposited Ti layer during this process compared to the bulk penetration distance of Ti in niobium makes it difficult to determine this distance inside grains exactly. To resolve this problem an additional diffusion experiment was performed in order to obtain the bulk (lattice) diffusion coefficient.

Thin Ti layers were deposited on the small Nb plates by RF sputtering from Ti mosaic target in an Ar gas atmosphere. Before the Ti deposition the Nb samples were pre-annealed for 5 hours at 1300ºC in primary vacuum (about $5 \cdot 10^{-3}$ mbar) in order to increase the grain size of niobium crystallites. It was done to minimise the influence of grain boundaries. There were prepared samples with two thickness of the titanium overcoat, 30 and 100 nm, measured by a profilometer. The samples were then annealed in the primary vacuum at 900, 1000, 1100 and 1200ºC for 6, 5, 5 and 2 hours, respectively.

Fig. 3.12 shows, as an example, two profiles obtained for the samples annealed at 1200ºC for 2 hours and at 1100ºC for 5 hours. The first sample was covered by 30 nm thick Ti layer while the second sample was covered by 100 nm thick Ti layer. The data are presented as the measured intensities of the ^{48}Ti and ^{93}Nb signals in the function of the sputtering time.

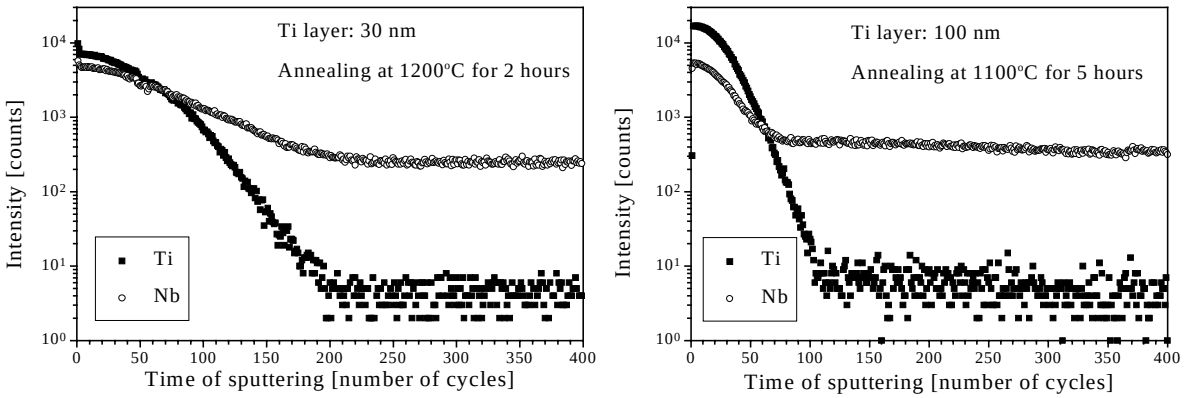

Fig. 3.12. An example of diffusion profiles presented in the form of the as measured isotopes intensities vs. the time of sputtering.

Fig. 3.13 presents the same data but in the form of the intensity ratio of the Ti and Nb signals, I(^{48}Ti)/I(^{93}Nb), in the function of the calculated depth. The former illustration does not allow determining easily the diffusion coefficient. The signals are not stable. This is caused by the sputtering effects like matrix effect. On the contrary to this, the latter way of presentation minimise these effects. Each profile for the samples with the thicker Ti layer (100 nm) consists of three parts. The first, having a high constant Ti/Nb signal, corresponds to

the still remaining Ti layer, the second part shows the decreasing concentration of the diffused Ti in Nb and the third part is the background level. For the samples with the thinner Ti layer (30 nm) the whole initial Ti quantity is diffused into niobium and the profiles consist of only two parts.

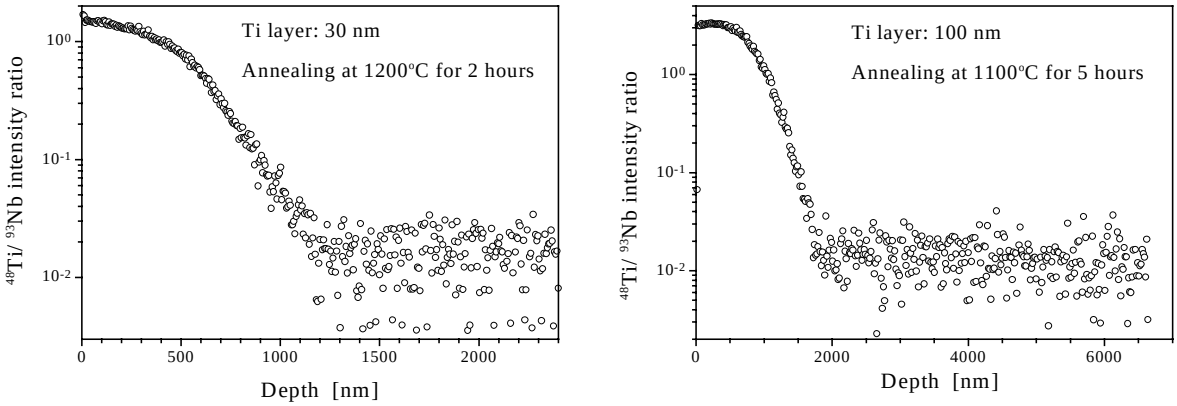

Fig. 3.13. The same profiles as in Fig. 3.12 but illustrated as the relative Ti and Nb intensities in the function of the calculated depth.

Assuming that the Ti/Nb intensity ratio is proportional to the concentration of Ti in Nb, it is possible to calculate the diffusion coefficient of titanium D_{Ti} from the sloping part of the I_{Ti}/I_{Nb} dependence.

The following gaussian low was used for calculations:

$$\frac{I_{Ti}}{I_{Nb}} \propto c_{Nb} = c_{Nb}^{0} \cdot \exp\left(\frac{-x^2}{4D_{Ti}t}\right). \qquad (1)$$

In this equation c is concentration, c^0 is the initial concentration, x is depth and t is the time of annealing.

The diffusion coefficient is determined from the slope of the line, obtained when presenting $\ln(I_{Ti}/I_{Nb})$ vs. x^2 (Fig. 3.14), which is equal to $-1/D_{Ti}t$. Thus calculated diffusion coefficients are presented in the Arrhenius plot (Fig. 3.15). The least square method allowed determining the temperature dependence of the diffusion coefficient, which is presented by the following equation:

$$D_{Ti} = 1.9 \cdot 10^{-7} \cdot \exp(-175\,\mathrm{kJmol^{-1}}/\mathrm{RT}) \quad [\mathrm{cm^2 s^{-1}}]. \qquad (2)$$

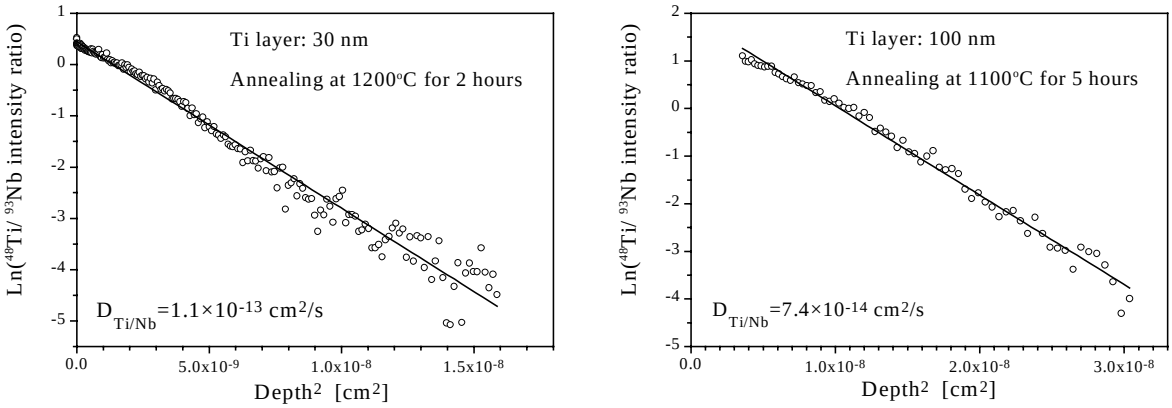

Fig. 3.14. Presentation of the sloping parts of the diffusion profiles from Fig. 13 as the logarithm of the Ti/Nb intensity ratio vs. square of depth according to equation (1).

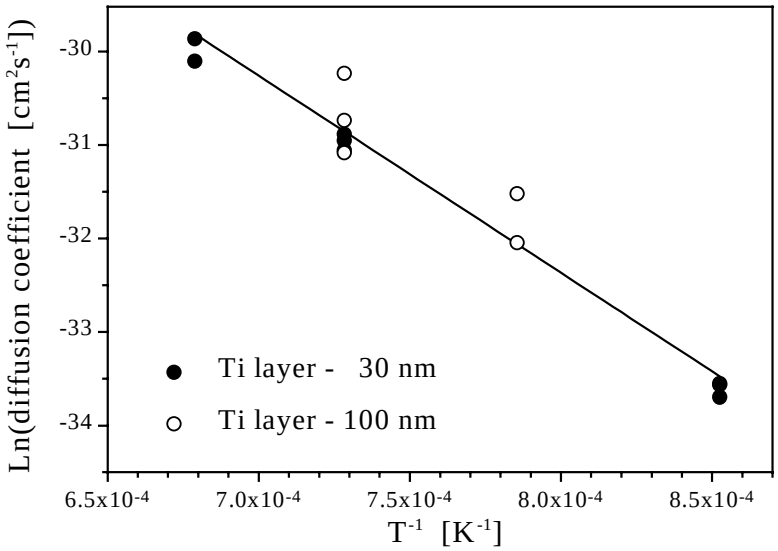

Fig. 3.15. Arrhenius plot of the determined diffusion coefficients.

The result obtained in this work differs from the literature data. In the paper by Pelleg[1] the Ti diffusion coefficient in niobium is described by the formula:

$$D_{Ti} = 0.99 \cdot 10^{-1} \cdot \exp(-368\,\mathrm{kJmol^{-1}}/\mathrm{RT}) \quad [\mathrm{cm^2 s^{-1}}].$$

In the article by Roux and Vignes[2] it is described by:

$$D_{Ti} = 0.4 \cdot \exp(-370\,\mathrm{kJmol^{-1}}/\mathrm{RT}) \quad [\mathrm{cm^2 s^{-1}}].$$

[1] *J. Pelleg, Diffusion of ^{44}Ti into Niobium Single Crystals, Philosophical Magazine, vol.21, no.172, April 1970, pp.735-41*

[2] *F. Roux and A. Vignes, Diffusion dans les systèmes Ti-Nb, Zr-Nb, V-Nb, Mo-Nb, W-Nb, Revue de Physique Appliquèe, Tome 5, June 1970, pp. 393-405*

The data of Pelleg were received for the radiotracer ^{44}Ti diffusion in the Nb monocrystals in the temperature range 994-1492ºC. As the serial sectionning technique anodizing and stripping methods were applied. Roux and Vignes have obtained their results in the interdiffusion experiments for the binary systems Ti-Nb by sintering together the pellets of Ti and Nb in the temperature range 1625-2075ºC. The interdiffusion profiles were determined on the cross-section of the sintered pellets perpendicularly to the front of the diffusion using the electron microprobe technique.

It is difficult to explain this discrepancy because the quality and the preparation of samples, the diffusion experiments and the methods of the profile determination were quite different in each work. However, for the temperature range from 1300 to 1500ºC the Ti diffusion coefficients calculated from the above three equations do not differ more than one order of magnitude what is a good estimation in this type of experiments.

3.5. Ti penetration paths in polycrystalline Nb samples.

Lateral titanium distribution in a function of depth was investigated for the TWC specimens treated at 800, 1000 and 1200°C. Subsequent maps obtained for the sample treated at 800°C show that titanium is not visible at grain boundaries (Fig. 3.16). It can be explained by higher Ti diffusion in this region. For the sample treated at 1000 and 1200°C this effect was not measured. It is probable that at the higher temperatures where the Ti diffusion increase, the contrast of the intensities between the grain boundaries and the grains was to weak to detect.

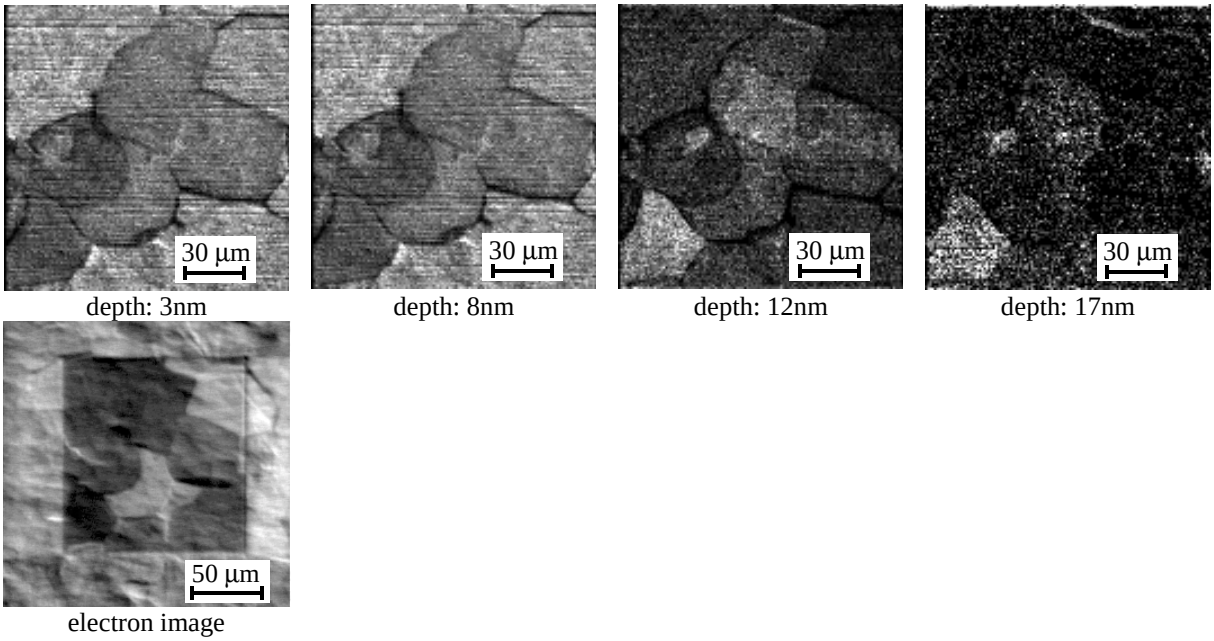

depth: 3nm | depth: 8nm | depth: 12nm | depth: 17nm

electron image

Fig. 3.16. Titanium composition maps at different depths measured by SIMS for the TWC sample treated at 800°C. Electron image presents the surface topography of the analysed area.

Transport of titanium into niobium was investigate using two series of samples. First series, here named A, was prepared in one cycle of treatment consisting of Ti deposition at 1350°C for 2h and then at 1400°C for 1h. The second series, named B, was prepared in two cycles of the same treatment. Each series contained 5 samples. First sample of each series were analysed as it was prepared.

The measurements in the grains indicated that the Ti layer is thicker for the sample treated in one cycle. The thickness of the layer for the not-etched sample A is about 7.5 µm but for the sample B can be estimated to about 6 µm (Fig. 3.17). Unfortunately, for these samples thickness of the Ti layer is too thick and investigation of fast diffusion paths could not be made with sufficient precision. Therefore, next samples were chemically etched in an acid mixture for 5, 10, 15 and 20 min respectively. The chemical etching rate of the Nb was

estimated to about 1 μm/min. Analysis of these samples showed that Ti penetration is deeper for the sample treated in two cycles. Titanium in the grains was not detected for the sample A etched for 5 min but it was measured for the sample B etched for the same time (Fig. 3.18).

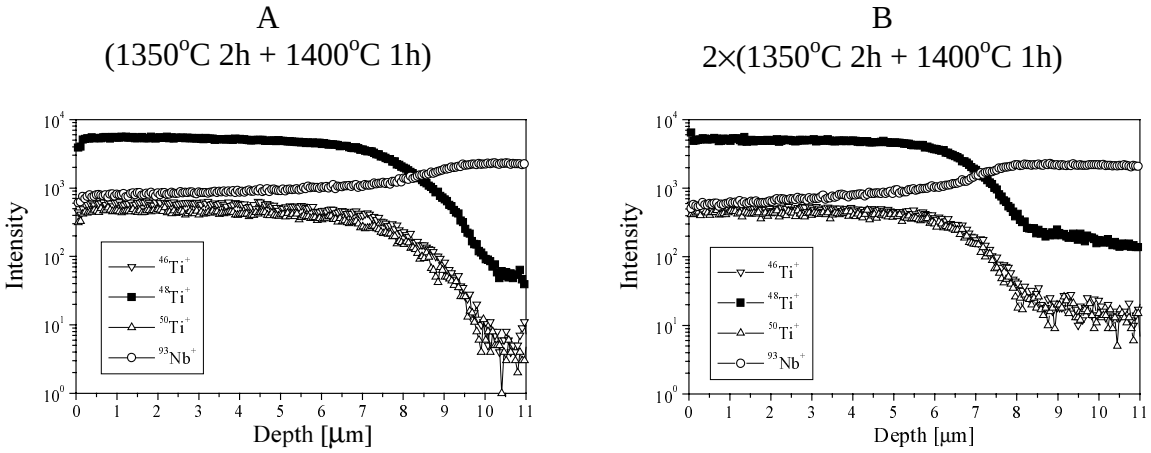

Fig 3.17. Depth profiles for the not chemically etched samples A and B.

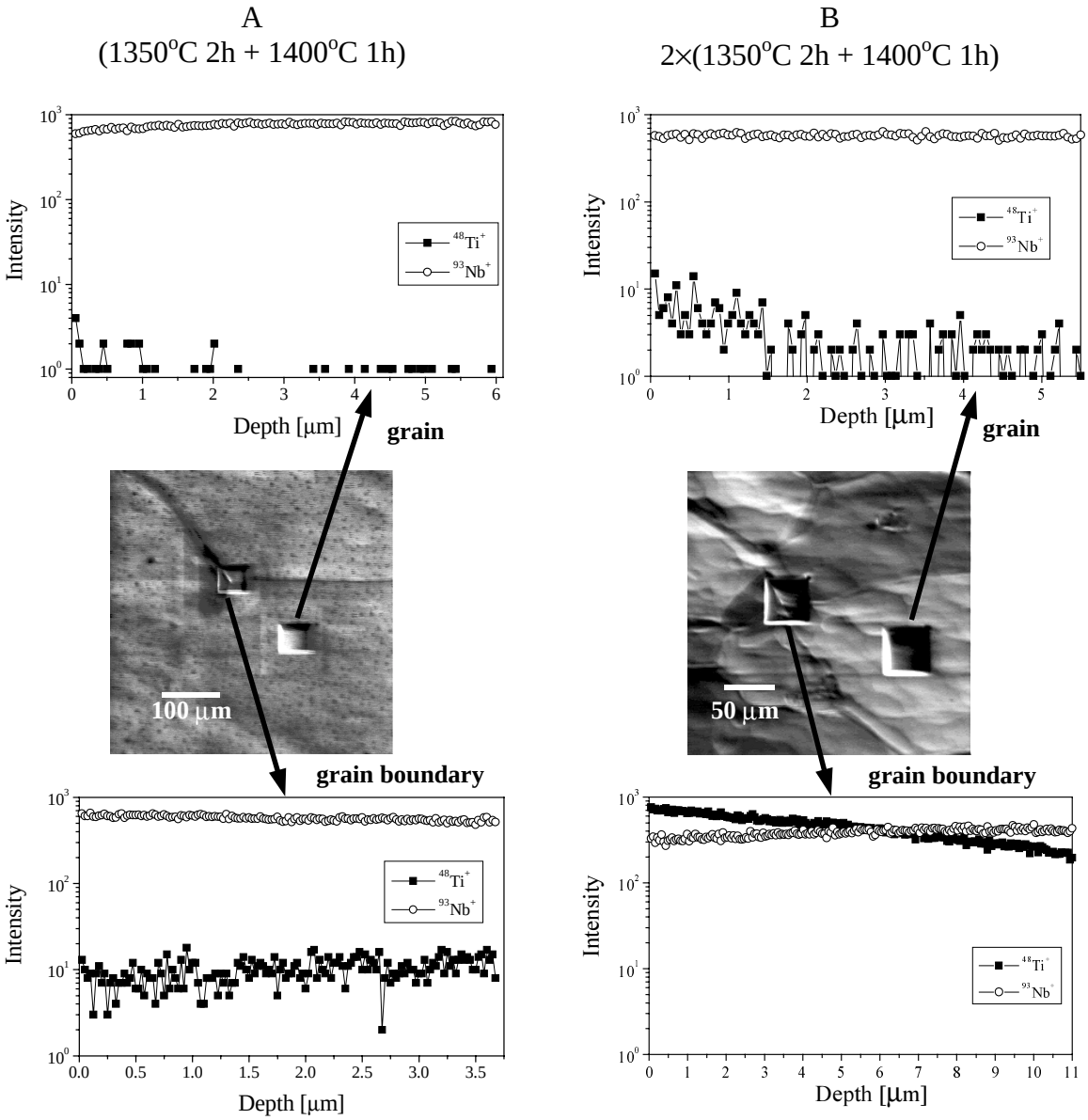

Fig 3.18. Depth profiles in the grains and in the grain boundaries for the samples A and B chemically etched for 5 min.

It was found that the titanium penetration depth is deeper in grain boundaries than in grains. This is illustrated in Fig. 3.18 where for the samples A and B chemically etched for 5 min the Ti intensity measured in the grain boundaries is much higher than in the grains. The range of the penetration along grain boundaries strongly depends on number of the preparation cycles (Fig. 3.19). For the sample A etched for 10 min Ti was not detected although several spots were analysed. On the contrary, even 20 min of etching of the sample B did not dissolved completely the layer penetrated by titanium.

time of etching [min]	A (1350°C 2h + 1400°C 1h)	B 2×(1350°C 2h + 1400°C 1h)
10	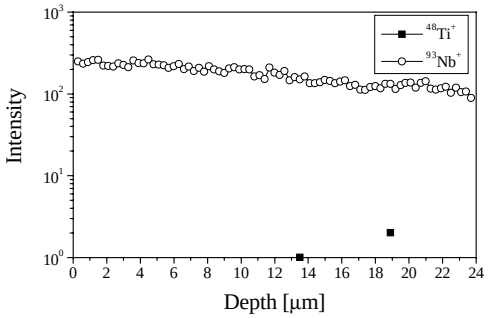	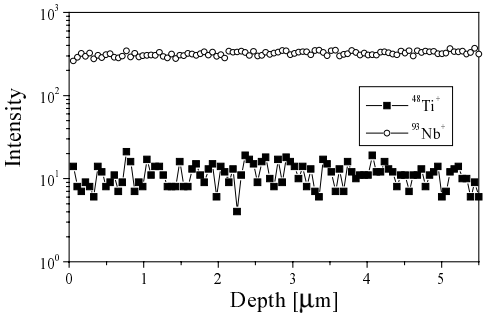
15		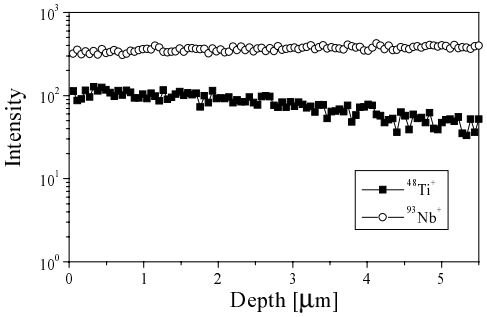
20		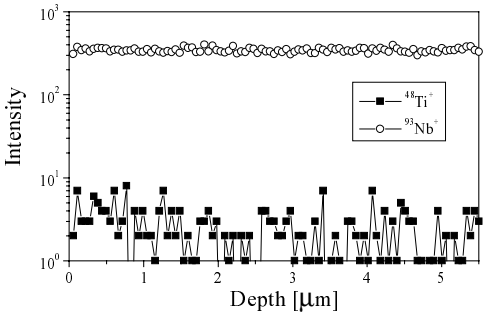

Fig. 3.19. Depth profiles in the grain boundaries for the samples A and B after chemical etching.

Precise observations of the Ti depth profiles in the grain boundaries for the sample B indicate that the Ti concentration depends not only on the depth but also on chosen area of grain boundaries. Composition maps measured for the chemically etched samples B (Fig. 3.20) show that titanium do not penetrate through the grain boundaries with the same rate.

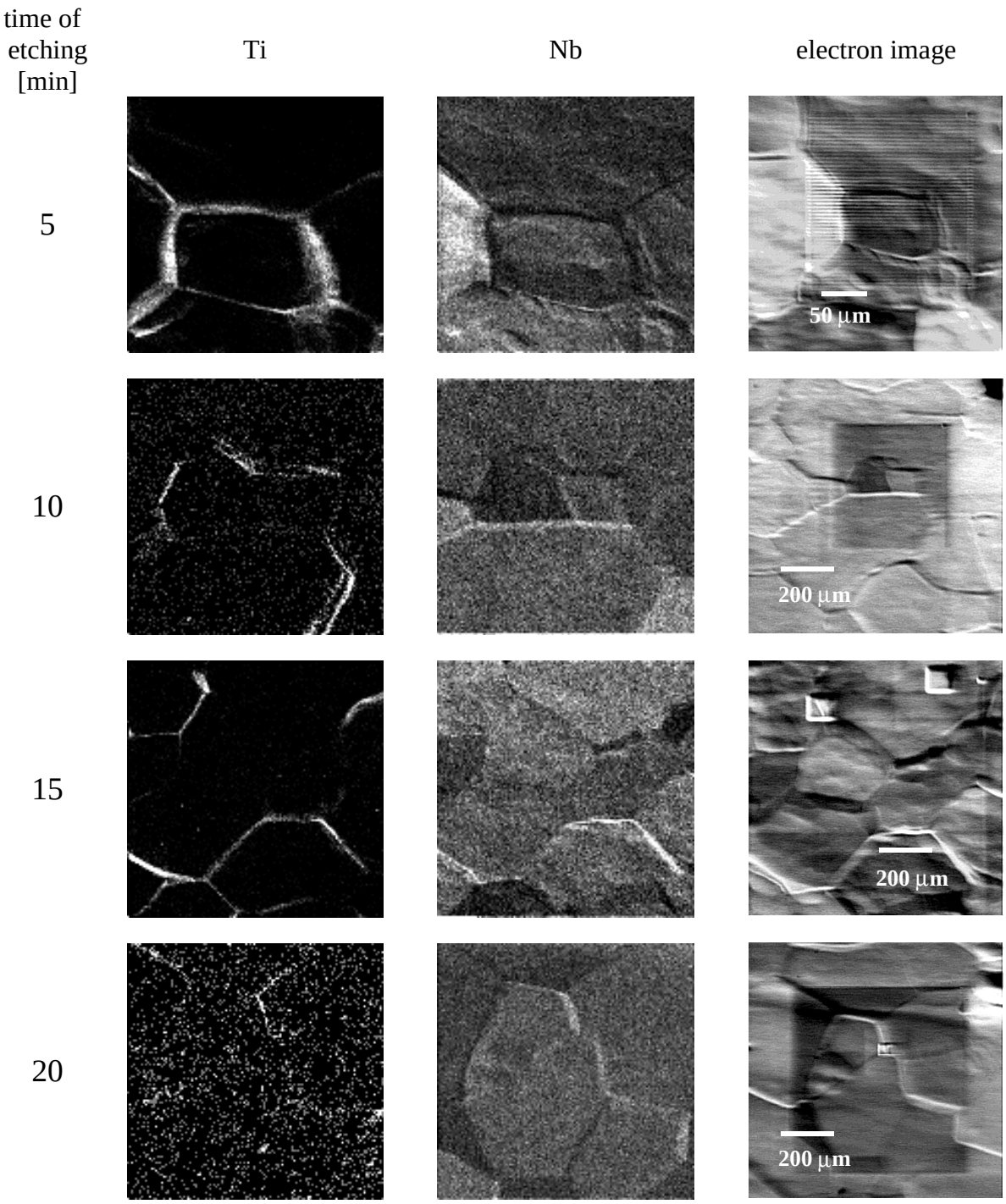

Fig. 3.20. Composition maps and electron images of the analysed areas for the samples of the series B chemically etched for different time.

Estimation of the absolute value of the penetration depth is charged by errors coming from sample preparation. In chemical profiling the main error is due to non-homogenous dissolution of the grains. Roughness of the sample surface increased with the time of the etching. Additionally the grain boundaries were strongly attacked and became broad and deep (Fig. 3.21). In the sputter profiling the sputter rate vary with grain orientations (Fig 3.22). Although both the dissolution rate and the sputter rate were determined separately it is not

possible too combine the depth scale. Taking into account the results of both methods the penetration range in the grain boundaries is shorter then 10 μm for the samples A and higher then 20μm for the sample B.

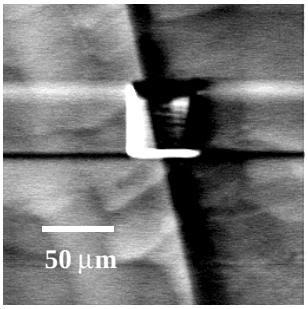

Fig. 3.21. Electron image of grain boundary for the sample B chemically etched for 20 min

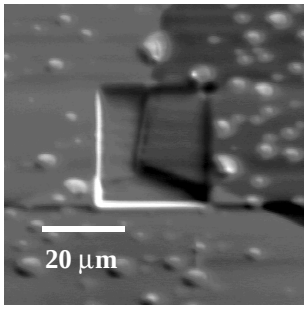

Fig 3.22. Electron image of triple point sputtered area for the sample series A.

4. Conclusions

The thickness of the Ti vapour deposited layer on pure niobium strongly depends on temperature and increases from 100 nm at 800^{o}C to about 20 μm at 1400^{O}C for the same time of 1 h. In this range of temperature the Ti diffusion into Nb was investigated. The Ti bulk diffusion coefficient was evaluated and can be expressed as:

$$D_{Ti} = 1.9 \cdot 10^{-7} \cdot \exp(-175\,\mathrm{kJmol^{-1}}/RT) \quad [\mathrm{cm^2 s^{-1}}].$$

The penetration range of titanium along grain boundaries is much deeper than in the grains. In the one standardised cycle of heat treatment (1350^{o}C 2h + 1400^{o}C 1h) it does not exceed 10 μm but in the double cycles it is higher than 20 μm. Titanium homogeneously covers the grains but its transport along the grain boundaries is non-uniform.